1 *Research Article*

2 # Butyl rubber-based composite: Thermal degradation
3 # and prediction of service life time

4 **Phuong Nguyen-Tri [1] *, Ennouri Triki[2], Tuan Anh Nguyen[3]**

5 [1] Department of Chemistry, University of Montreal, Montreal, Quebec, Canada;
6   phuong.nguyen.tri@umontreal.ca
7 [2] Department of Mechanical Engineering, McGill University, Montreal, Quebec, Canada;
8   ennouri.triki@mail.mcgill.ca
9 [3] Institute for Tropical Technology, Vietnam Academy of Science and Technology (VAST), Hanoi 122100,
10   Vietnam; ntanh2007@gmail.com
11
12 * Correspondence: phuong.nguyen.tri@umontreal.ca ; Tel.: + 514-340 5121 (7326)

13

14 **Abstract:** Butyl rubber-based composite (BRC) is one of the most popular materials for the
15 fabrication of protective glove against chemical and mechanical risks. However, in many working
16 places such as metal manufacturing or automotive mechanical services, its mechanical hazards
17 usually appear together with metalworking fluids (MWFs). The presence of these contaminants,
18 particularly at high temperature, could modify its properties due to the scission, the plasticization,
19 the crosslinking of polymer network and thus led to severe modification of mechanical and
20 physicochemical properties of material. This work aims to determine the effect of temperature and
21 a metalworking fluid on mechanical behavior of butyl rubber composite dealing with crosslinking
22 density, cohesion forces and elastic constant of BRC on the based on Mooney-Rivlin's theory. The
23 effect of temperature with and without MWFs on thermo dynamical properties and morphology of
24 butyl membranes is also investigated. The prediction of service lifetime is then evaluated from
25 extrapolation of Arrhenius plot at different temperatures.

26 **Keywords:** Polymer aging, swelling behavior, protective glove materials, elastomers, composites,
27 rubber

28
29

1. Introduction

31 Rubber is one of the most important materials for various industries, especially in petroleum,
32 construction [1] and protection material sectors [2, 3]. Protective gloves are often covered by an
33 elastomeric coating to protect against chemical and mechanical damages due to its good resistance to
34 abrasion, oils, chemicals and its excellent damping properties [4-12]. However, the swelling
35 phenomena involving the degradation of the mechanical properties of these materials have often
36 been observed [13]. Butyl rubber-based composite (BRC) is one of the most effective materials against
37 chemical risks [4, 13]. However, this material is sensitive to nonpolar solvents or metalworking fluid.
38 These non-polar compounds can easily penetrate in the polymer and lead a dramatically change of
39 material properties. These problems represent a large risk for users and thus require a better
40 understanding of the problem [13, 14]. Like other polymers, butyl rubber-based composites can be
41 affected by oxidation and this effect becomes more intensive at high temperature.

42

43   The swelling characteristics of rubbers are related to the deterioration of mechanical properties
44 and may affect to their failure mechanics. Nowadays, there are no models to predict the failure

45 mechanisms in the presence of industrial contaminants. Several investigations have been reported on
46 the effect of industrial contaminants on morphology, mechanical properties and structure of gloves
47 material. In previous works [15-24], we reported that polymers and composites [16-20, 22, 23, 25-41]
48 can be degraded by several aging agents such as heat, water, humidity, oxygen, ozone and various
49 other environments factors [16-24]. The scission, crosslinking and plasticization of polymer network
50 may be occurred and led to severe deterioration of mechanical and physicochemical properties of
51 material [42], which are quite important as regards their applications in various fields of mechanical
52 engineering.
53

54   Many researchers have been attempted to understand the relationship between morphological
55 and property changes with microstructure of rubber material[43], especially with failure mechanism
56 of elastomer by using several traditional test methods including tensile test, strain-stress relation, and
57 compression measurements [44-46]. Mooney-Rivlin's equation is usually used to evaluate the
58 property-structure relationship of material by analysing of tensile stress-strain curves of materials. In
59 this model, Rivlin [47, 48] proposed an extension of the Mooney's model by describing W as a
60 polynomial series in (I_1 - 3) and (I_2 - 3):

61
$$W = \sum_{i.j=0}^{\infty} C_{ij} \left(I_1 - 3 \right)^i \left(I_2 - 3 \right)^j \quad \text{with } C_{00} = 0 \qquad \text{Eq.1}$$

62 During a simple tensile test, we are:

63
$$I_1 = \lambda^2 + \frac{2}{\lambda} \qquad\qquad I_2 = \frac{1}{\lambda^2} + 2\lambda \qquad\qquad I_3 = 1 \qquad \text{Eq.2}$$

64 The stress σ_n is given by the equation:

65
$$\sigma_n = 2\left(\lambda - \frac{1}{\lambda^2} \right)\left[\frac{\partial W}{\partial I_1} + \frac{1}{\lambda} \frac{\partial W}{\partial I_2} \right] \qquad \text{Eq.3}$$

66 According to the behavior law, we can still write:

67
$$\sigma_n = \lambda \frac{\partial W}{\partial \lambda_1} + \frac{1}{\lambda} \frac{\partial W}{\partial \lambda_2} \qquad \text{Eq.4}$$

68 From which

69
$$\sigma_n = 2\left(C_1 + \frac{C_2}{\lambda} \right)\left(\lambda - \frac{1}{\lambda^2} \right) \qquad \text{Eq.5}$$

70 where W is the density of deformation energy, λ is elongation of material and C_1 et C_2 are two elastic
71 constants associated with network structure and the flexibility of network, respectively. According
72 to Eq.5, plot of $\sigma_n / 2\left(\lambda - 1/\lambda^2 \right)$ as a function of λ^{-1} should be a linear and the C_1 constant is directly
73 calculated by extrapolating of the linear portion of the curve up to $\lambda^{-1} = 0$ and the C_2 constant is the
74 curve slope. In the molecular aspect, this constant C_1 of Mooney-Rivlin's model characterizes by the
75 density of crosslinking between elastomer chains [49, 50]. It can be used to evaluate the physical
76 manifestation of the degree of crosslinking N [51, 52].

77

78
$$N = \frac{2C_1}{kT} \qquad\qquad \text{Eq.6}$$

79 The constant C_2 is associated with the cohesion forces (intramolecular bonds and interchain) and
80 reinforcement-matrix interactions[52]. This constant also reflects the flexibility of the structure of the
81 material[53]. It depends on the degree of vulcanization which increases with the increasing of the
82 crosslink density[53]. The values of two constants C_1 and C_2 that can be determined during the tensile
83 tests allow for studying the influence of the crosslinking degree and network structure on the stiffness
84 of material. Gordon [52] is determined the Young's modulus according to C_1 and C_2:

85
$$E = 6\left(C_1 + C_2\right) \qquad\qquad \text{Eq.7}$$

86 It reported that the constant C_1 usually remains constant with variation of the swelling degree
87 of polymer material, while the constant C_2 decreases with the increase of swelling degree[54-56]. It
88 lacks a systematically research on the effect of temperature and metalworking on morphology,
89 properties and structure of elastomer materials.
90 In this study, a butyl rubber membrane, representing a common material used in protective
91 gloves, has been used to determinate the swelling characteristics to metalworking fluid at various
92 temperatures ranging from 80 °C to 120 °C. The elastic behaviors dealing with elastic constants,
93 crosslinking density and modulus were continuously followed during the contamination procedure
94 to evaluate the dominant parameter on polymer deterioration. The modification of morphology,
95 tensile properties and physicochemical properties were also investigated.

2. Materials and Methods

96

97 *2.1. Materials*

98 Butyl rubber based composite (BRC) membranes used in this work are made from butyl rubber
99 with carbon black fillers. These commercial products (thickness of ~1.6mm) are kindly supplied by
100 MCMaster-Carr Inc. (Canada). An industrial MWF used in this work, namely Milform 64 SST, is
101 directly purchased from a company in metalworking sector in Quebec, Canada. The chemical
102 composition can be found in our previous publication. The carbon black filler content in composite
103 membranes is estimated to be 42- 44 wt.% (by TGA measurement).

104 *2.2. Contamination procedure*

105 The elastomer membranes having the mass (m_0) were immersed in to the liquid contaminants
106 for different periods of time for measuring of swelling index changes according to the ASTM D471-
107 12 standard. They are then delicately wiped by thick wiping papers to remove the excess oil on
108 sample surface and reweighed (m_t). The process is repeated until saturated state. The swelling index
109 (M) is calculated according to the relation following:

110
$$M(\%) = \frac{m_t - m_0}{m_0} x100 \qquad\qquad \text{Eq.8}$$

111 where m_0 and m_t are respectively the weight of the samples before and after immersion in
112 contaminant.

113 *2.3. Scanning electron microscopy (SEM)*

114   Scanning electron microscopy model Hitachi S570 was used to investigate the morphology and
115   the fractography changes of samples before and after contamination process. These observations
116   serve to examine the failure modes of morphology changes of elastomer materials.

117   *2.4. Tensile tests*

118   Tensile properties of elastomer membranes are measured with the dog bone rectangular
119   samples. Measurements were performed with an Alliance 2000 (MTS) universal testing machine
120   equipped with 1000N load cell and operated at a cross-head speed of 500 mm/min according to the
121   ASTM D412-06 standard test method. For each condition, five replicates are measured.

122   *2.5 Thermal gravimetric analysis (TGA)*

123   TGA is carried out with original and aged composite samples to evaluate the percentage of filler
124   content and the effect of aging process on the sample weight loss as a function of time. The TGA is
125   carried out in nitrogen atmosphere at a heating rate of 20 ºC/min using a Parkin Elmer TGA model
126   4000. Thermograms were recorded from 0 to 800 ºC.

127

128   **3. Results and discussions**

129   *3.1. Effect of temperature on mechanical properties*

130   The influence of temperature on the viscoelastic properties of BRC is investigated at three
131   different temperatures ranging from 80 and 120°C. Figure 1a shows the relationship between the
132   constant C_1 and exposure time. It demonstrates that the highest value of constant C_1 is observed at
133   temperature around of 120°C. At the beginning of exposure (t < 4 h), C_1 undergoes a significant
134   increase, and then rapidly decreases before achieving a constant value. At lower exposure
135   temperature (80°C and 100°C), the variation of the constant C_1 is not significant representing by a
136   slight decrease of C_1 at the first exposure hours then appears to be converged to the similar value to
137   that observed at 120°C. These results allow confirming that the stiffness of butyl is optionally
138   increased with temperature, as reported in the case of a neoprene membrane which is exposed to
139   high temperature [57]. Figure 1b shows the variation of C_2 as a function of exposure time at different
140   temperatures. The variation of the constant C_2 at 80°C appears to be similar to that at 100°C with
141   parabolic shape curve. An increase in C_2 at first hours of exposition (t < 4h) is observed and then it
142   becomes to slightly decrease with the time. It can be attributed to the increase of cohesive force at the
143   first hours of exposition time and then decrease [54]. This physical phenomenon is completely
144   different to that observed at higher exposure temperature (120°C). The constant C_2 decreases
145   significantly from the first steps of exposure and go down to zero. These results are not surprise and
146   are in good agreement with that published by Marck [54].

147
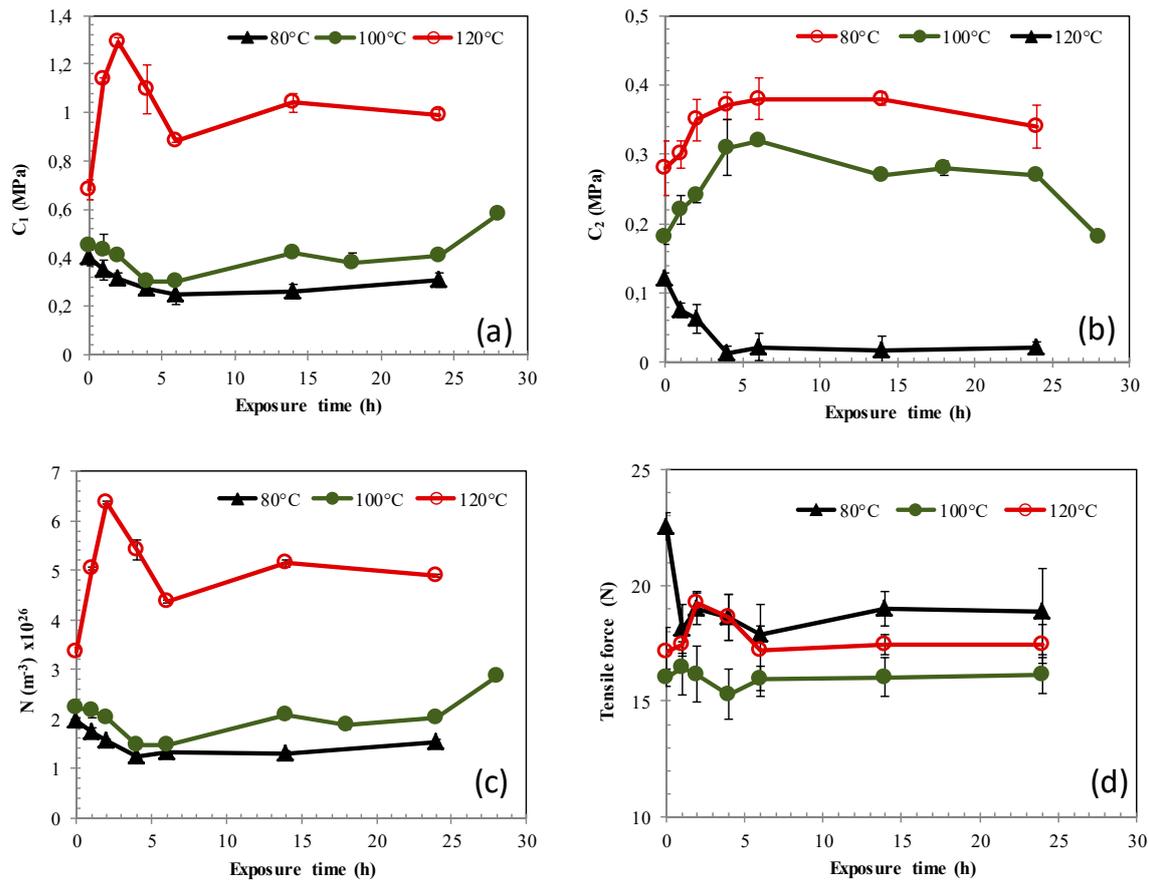
Figure 1 Effect of temperature on mechanical properties of BRC as function of MWF exposure time a) constant C_1; b) constant C_2; c) Crosslinking density (N); d) Tensile force.

The synergy the between the variation of C_1 and C_2 is also investigated and the results are shown in Table 1. This synergy is determined by calculating the theoretical Young's modulus by using Eq.7 and the experimental Young's modulus from the first linear region of the force-displacement curves (Fig. 1d). The obtained results show that the rigidity of the butyl remains almost unchanged at 80°C. However, a significant increase of Young's modulus with exposure time was recorded at 100°C and 120°C. This can be attributed generally to the increasing of crosslinking density (N) that may be occurred at high temperature due to the vulcanization or reticulation of polymer chains. After 24 hrs exposure in MWF, the Young's modulus seems to be increased for all studied temperatures (Fig 1c). Figure 1d demonstrates the tensile force of BRC as a function of exposure time, it can be seen that the rupture properties remain constant during all exposure times whatever the exposure temperature. The variation of tensile strength at break with exposure time is not significant. This implies that the BRC has relative high resistance to temperature for a short time and the later does not affect the mechanical failure behavior.

171   **Table 1:** Young Modulus values of a butyl membrane exposed various temperatures

172

173

Exposure time (h)	Exposure temperature					
	80°C		100°C		120°C	
	E_{theo}	E_{exp}	E_{theo}	E_{exp}	E_{theo}	E_{exp}
0	4.08	3.40	3.78	3.00	4.80	4.11
	(0.42)	(0.04)	(0.06)	(0.05)	(0.30)	(0.16)
1	3.90	2.89	3.93	3.15	6.57	6.10
	(0.36)	(0.2)	(0.48)	(0.25)	(0.12)	(1.10)
2	3.99	3.01	3.90	3.20	8.12	7.43
	(0.30)	(0.09)	(0.10)	(0.13)	0.24)	(0.18)
4	3.78	2.99	3.66	2.88	6.65	5.45
	(0.24)	(0.03)	(0.36)	(0.18)	(0.66)	(0.85)
6	3.78	2.98	3.72	3.01	5.44	4.57
	(0.42)	(0.10)	(0.04)	(0.02)	(0.18)	(0.02)
14	3.84	2.98	4.14	3.27	6.35	5.08
	(0.24)	(0.09)	(0.09)	(0.01)	(0.36)	(0.14)
24	3.90	2.96	4.08	3.30	6.08	4.80
	(0.36)	(0.02)	(0.09)	(0.09)	(0.16)	(0.12)

174   Note: between parentheses: standard deviation (SD)

175

176   *3.2. Effect of simultaneous temperature and metalworking fluid on properties, structure and morphology*

177   In the working condition, glove materials are often in contact with hot MWFs, generated by
178   friction of machine devices. This factor could be directly affected on the protective performance of
179   the glove materials. The effect of simultaneous temperature and MWFs on properties of butyl
180   membranes is investigated. Figure 2a shows the variation of the constant C_1 as a function of expose
181   temperature in the presence of a metalworking fluid (Milform 64 SST). As shown in Figure 2a, the
182   changes of the constant C_1 with exposure time at 80°C are substantially similar to that at 100°C, thus
183   these two curves are approximately superposed. However, at 120°C, the curve tendency is different
184   when compared to that at lower exposure temperatures, where C_1 values dramatically drop at the
185   first hours of exposure and then tends to archive a plateau region. Figure 2b shows the effect of
186   temperature and MWFs on the constant C_2. It demonstrates that the constant C_2 is rapidly decreased
187   with the exposure time and approach to zero after 24 hrs of exposition. Therefore, the cohesive
188   strength of inter-chain eventually became weak [54] and the viscoelastic behavior may be also
189   affected. The results are in good agreement with that observed by Gumbrell *et al.* [58] and Allen *et*
190   *al.[59]* in studying the aging process of natural rubber to different solvents.

191

192   The calculation of the Young's modulus, in particular at 80 °C and 100 °C, highlights the effect
193   of simultaneous temperature and contaminants on the rigidity of the material. A significantly
194   decrease of Young's modulus as a function of exposure time was observed (Table 2). This could be
195   attributed to the reduction of the cohesive strength of inter-chains. The rigidity of butyl at 120°C is
196   unstable. The Young's modulus firstly increases, then decreases before achieving a plateau region.

197 This variation is possibly related to the changes in the cross-linking density (N) as shown in Figure
198 2c. This variation is due to the correlation between the constants C_1 and C_2. The similar behavior was
199 also discussed by Nohilé et al.[4] demonstrating that the swelling of BRC by solvents led to an
200 increase of the material rigidity due to the loss of fillers. The later leads to a reduction of the tensile
201 strength of BRC as shown in Figures 2d. It can be seen from these figures that the mechanical
202 properties of material are decreased whatever exposure temperatures are applied. The longer
203 exposure time, the higher loss of mechanical is observed.

204
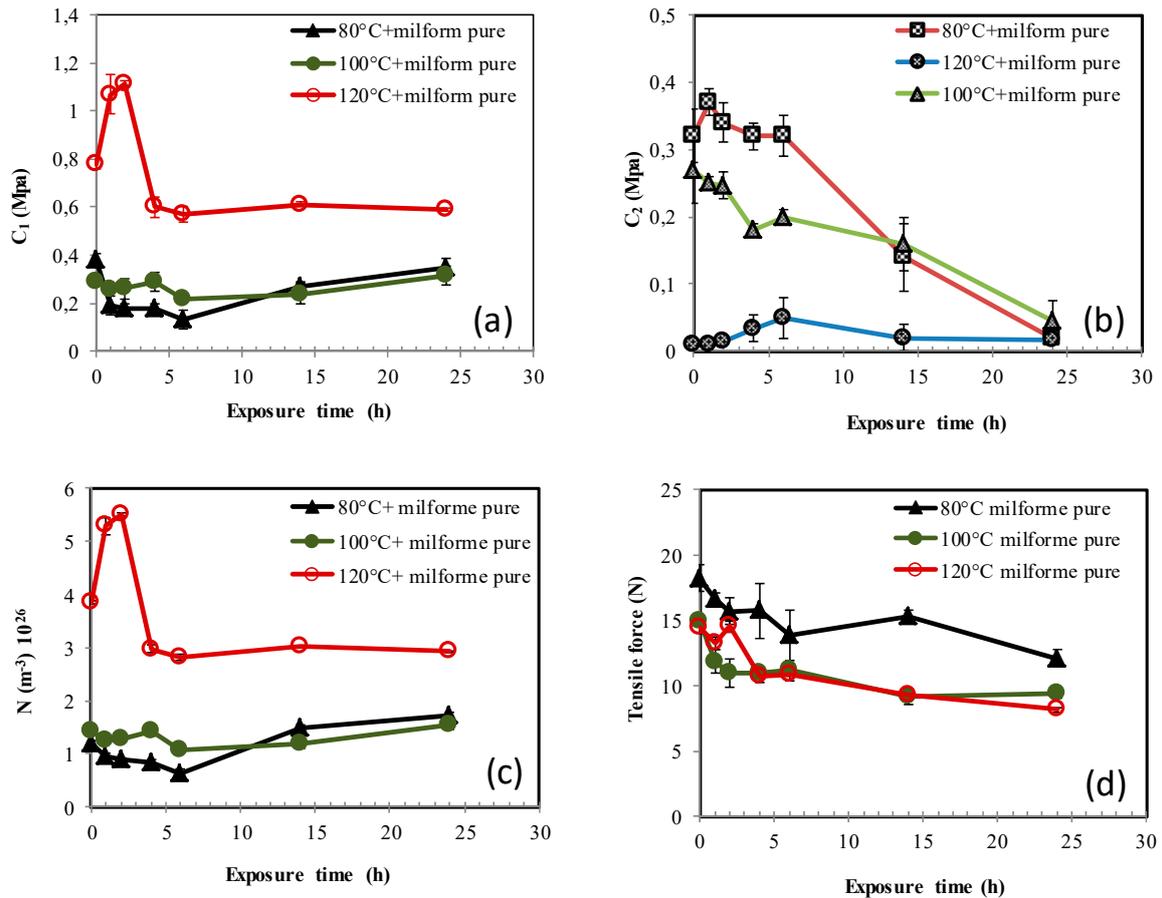
205

206 **Figure 2** Effect of temperature and a MWF on mechanical properties of BRC as function of MWF
207 exposure time a) constant C_1; b) constant C_2; c) crosslinking density (N); d) tensile force.

208
209
210
211
212
213
214
215
216
217
218

219 **Table 2:** Young Modulus values of BRC membrane exposed at different temperatures in the presence of
220 metalworking fluid

221

t (h)	Exposure temperatures					
	80°C		100°C		120°C	
	E_{theo}	E_{exp}	E_{theo}	E_{exp}	E_{theo}	E_{exp}
0	3.72	2.87	3.36	2.70	4.74	4.26
	(0.36)	(0.20)	(0.36)	(0.22)	(0.15)	(0.28)
1	3.36	2.64	3.03	2.51	6.76	6.28
	(0.36)	(0.16)	(0.12)	(0.09)	(0.54)	(0.17)
2	3.12	2.43	3.03	2.52	6.78	6.46
	(0.30)	(0.08)	(0.20)	(0.01)	(0.09)	(0.01)
4	3.00	2.41	2.82	2.33	3.804	3.26
	(0.24)	(0.05)	(0.30)	(0.11)	(0.36)	(0.18)
6	2.70	2.30	2.52	2.18	3.72	3.41
	(0.42)	(0.03)	(0.12)	(0.03)	(0.36)	(0.03)
14	2.46	2.31	2.40	2.01	3.66	3.15
	(0.24)	(0.05)	(0.48)	(0.05)	(0.18)	(0.04)
24	2.22	1.98	2.16	1.92	3.64	3.06
	(0.36)	(0.02)	(0.42)	(0.06)	(0.04)	(0.05)

Note: between parentheses: standard deviation (SD)

222 *3.3.   Effect of temperature and MWF on dynamical Thermo-mechanical properties*

223   Dynamical thermo-mechanical analysis (DMTA) provides access to the elastic modulus and
224 tangent values of materials. Figure 3a shows the example of Young modulus of BRC membrane
225 before and after aging at 100 °C during 24 h in MWF (Milform 64SST). The curves are recorded from
226 temperature -120 °C to 70°C. It shows that thermal degradation of membrane in metalworking fluid
227 significantly reduces its Young modulus. It is clearly seen that the Young modulus is decreased from
228 1.45×10^7 to 4×10^6 MPa at -120 °C after aging at 100 °C for 24 h of exposure.

229
230
231
232
233

234
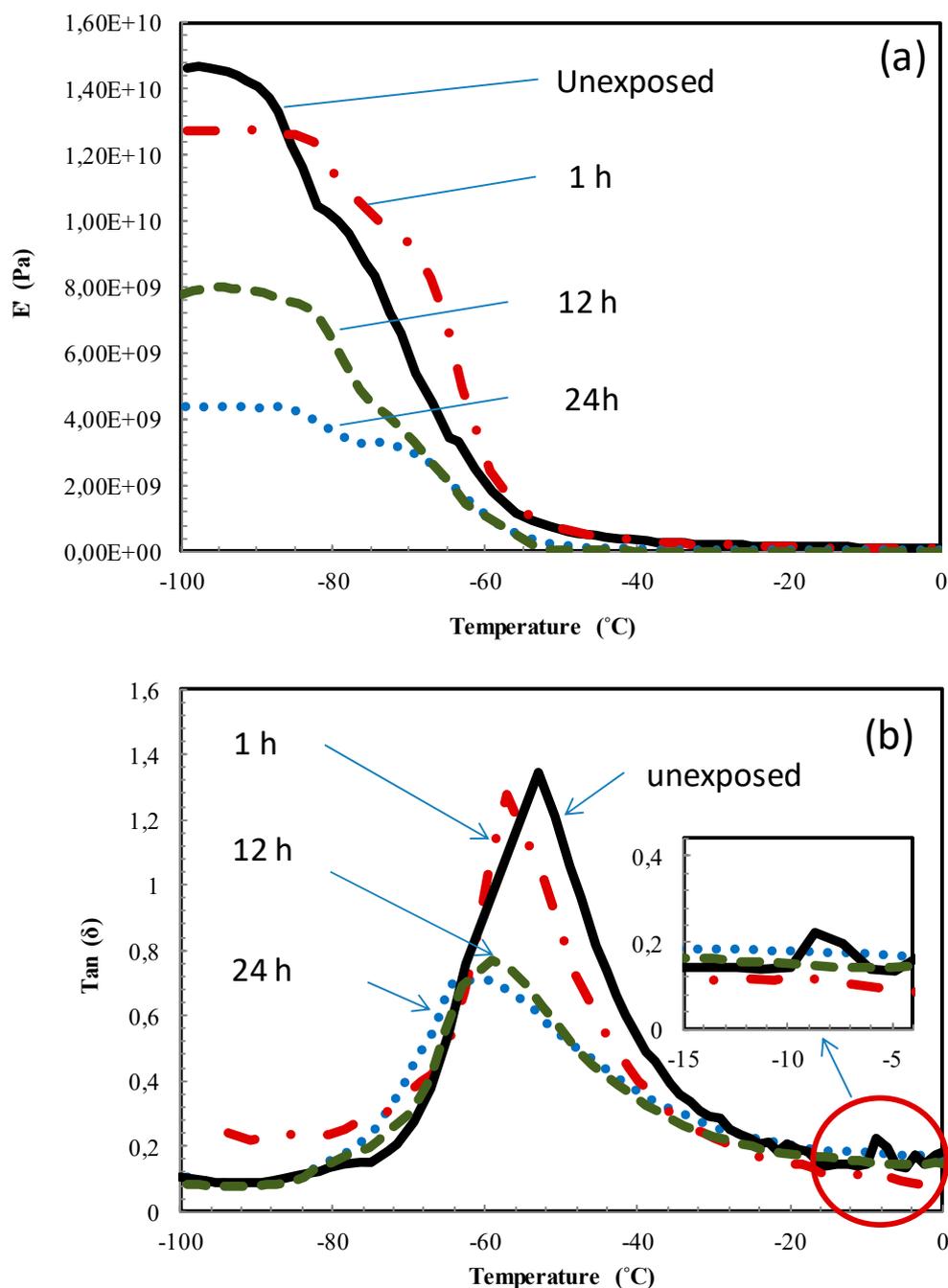
Figure 3 Evolution of storage modulus (a) and tangent delta values (b) of butyl rubber composite membrane before and after exposure in metalworking fluid (Milform 64 SST) at 100 °C during 24 h.

237

238   For an elastomer material, the glass transition temperature (T_g) is important factor that directly involves to the final properties of materials. This parameter is directly determined by DMTA curves, corresponding to the maximum peak of tan (δ). Figure 3b shows the example of the variation of tan (δ) of aged and un-aged samples at 100 °C with different aging times. It can be seen that the curve has a transition located around at - 45 °C, due to the glass transition temperature of butyl rubber. Another peak at a higher temperature at -8°C was also observed. This may be associated to movement of local molecular relaxations side [60, 61]. These local molecular movements not only affect the

245 viscoelastic response, but also the mechanical properties (elastic modulus, plastic deformation) and
246 also the diffusion of solvents in polymer matrix.

247   After aging at 100 °C in a metalworking fluid (Milform 64SST) for 24 h, a significant increase of
248 the glass transition temperature value from - 45 °C to - 63 °C temperature was observed. This result
249 is in good agreement with that in the literature in showing that there was a decrease of T_g of BRC
250 during thermal aging in silicone oil [62]. The intensity of tan peak (δ) of aged sample is observed to
251 be lower than that of the un-aged sample. The disappearance of the peak corresponding to the
252 secondary transition temperature associated with the local molecular movement is observed in the
253 aged sample. It can be attributed by the presence of MWF in elastomer matrix and leads to a better
254 "molecular lubrication" due to the plasticization affect [63].   Regard to the reduction of T_g, since the
255 glass transition temperature varies linearly with the molar mass and the molecular loss lead to a shift
256 of the T_g to lower temperature areas [64]. The decrease of T_g observed this present study, is may be
257 due to the thermal and chemical degradation of material by chains scissions that lead to a reduction
258 of the molecular mass, that can explain the deterioration of mechanical properties of the material as
259 shown in the previous section.

260

261 *3.4.   Effect of temperature and MWF on morphology, thermal properties and service lifetime of butyl*
262 *composites*

263   The scanning electron microscope was used to study the changes of the BRC membrane
264 morphology during aging process. Figure 4 shows the SEM images of a sample of butyl before and
265 after exposure in MWF. Figure 4 d shows that in the case of unexposed sample, a large distribution
266 of fillers in the elastomer matrix is observed. However, these reinforcements are missing at the
267 surface of exposed sample. The appearance of holes on the surface of the aged sample is also
268 observed, this can be due to the removal of fillers that replaced by metalworking fluid (Fig. 4b). In
269 other studies, the same damage was observed with bromobutyl rubber when they are undergone a
270 thermal aging process [65]. The presence of MWF at elevated temperature, various micro cracks on
271 the exposed sample (Fig. 4c) can be found due to the loss of reinforcements at the sample surface,
272 generated by thermo-oxidation aging and plasticization effect. This observation is in good agreement
273 the literature [65]. The appearance of micro-cracks on rubber materials is believed to derive from the
274 nucleation effect of the dissolved vapor and gas in the low molecular weight domains of the rubber
275 [66]. The loss of reinforcement is confirmed by thermogravimetric analysis (TGA) under argon
276 atmosphere conditions. The thermal stability of BRC membrane was evaluated by thermo
277 gravimetric analysis at the temperature range from 30 to 800°C (Figure 5). The TGA curves show that
278 the decomposition BRC evolves in the same way for both aged and un-aged samples. It found that
279 the onset decomposition temperature of an original sample is about 205 °C with a residue of 52 % at
280 460 °C while the onset decomposition temperature for the aged one is about 228 °C with a residue of
281 42 % at 460 °C. In other words, the aged process leads to a reduction of carbon black filler from 52 %
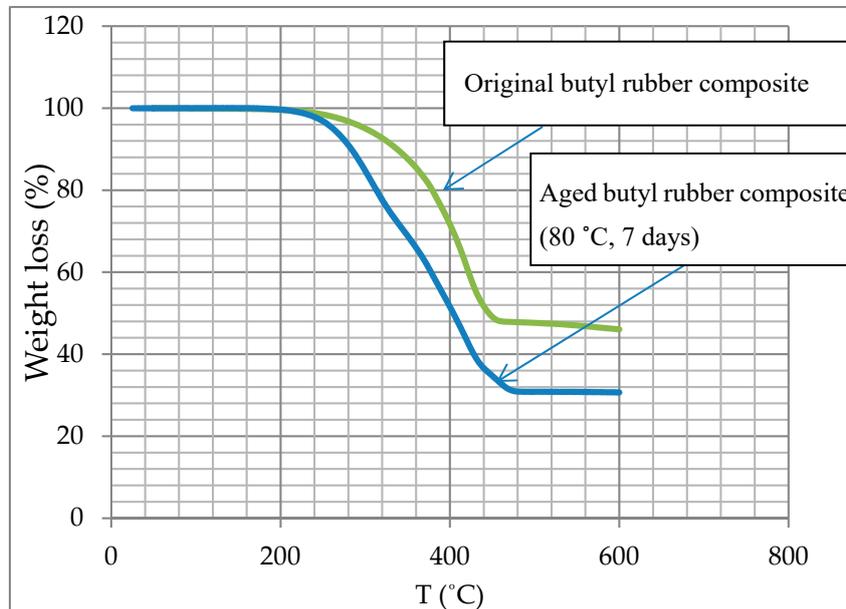282 for original rubber to about 42 % for aged sample.

283

284
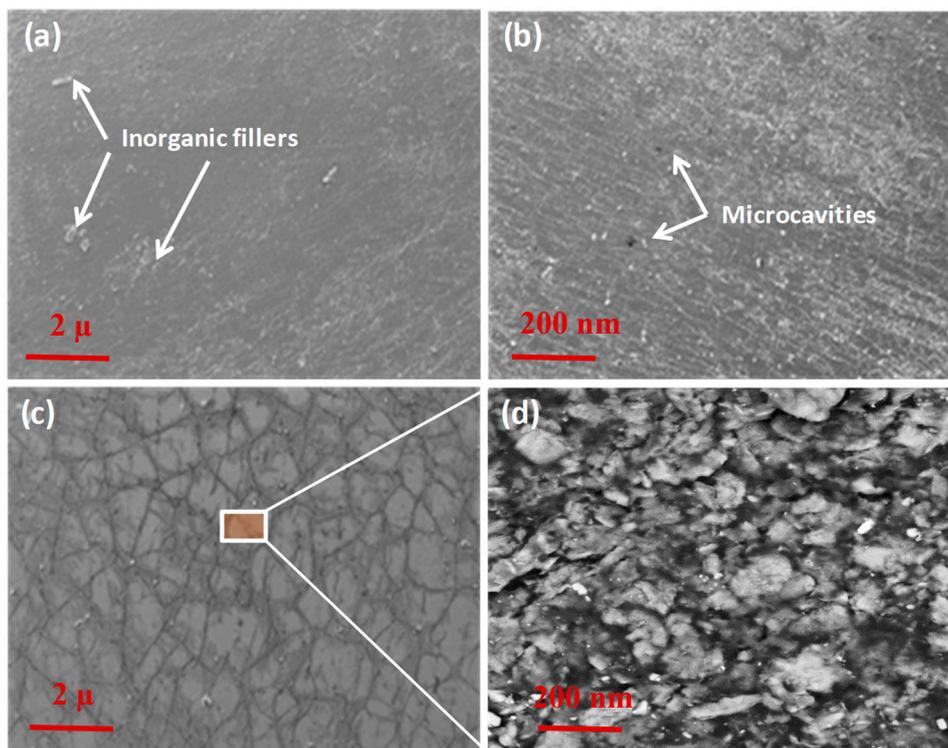
Figure 4   SEM images of butyl rubber composite membranes: a) non-aged sample, b) aged at 100 C, c) aged at 100 °C with the presence of a metalworking fluid (Milform 64 SST) during 24 hrs, c) higher magnification of image 4c, showing the rugosity of sample surface.


Figure 5   Thermogravimetric curves of butyl rubber composite before and after aged in Milform 64 SST at 80 °C during a week.

297   Changes in tensile force are observed at all studied temperatures (Figure 6). Indeed, after 24 hrs
298   of exposure, the tensile force drops by about 23 % at 80 °C. Whereas it decreases by about 41 % at 120
299   °C. The results of tensile tests of BRC at different temperatures helps to give a prediction of the service
300   life out by applying the Arrhenius model to the time-temperature data (Eq.9). In fact, the variation of
301   rate of overall aging processes can be calculated from mentioned above equation (Eq.9). Where E is
302   activation energy, R is universal constant (8.314 J/mol.K), T is absolute temperature and A is the pre-
303   exponential factor. The curves describing the relationship between ln(t) vs 1/T should be linear and
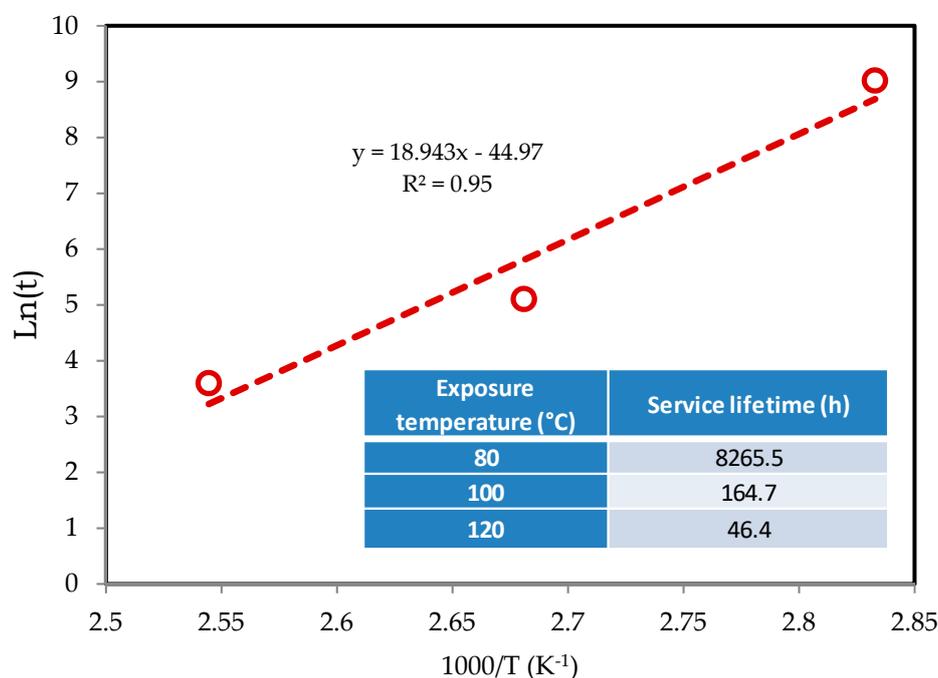304   thus the activation energy and service life time can be calculated from this curve.
305
306                              $K = A \exp(-E/RT)$ Eq.9
307
308
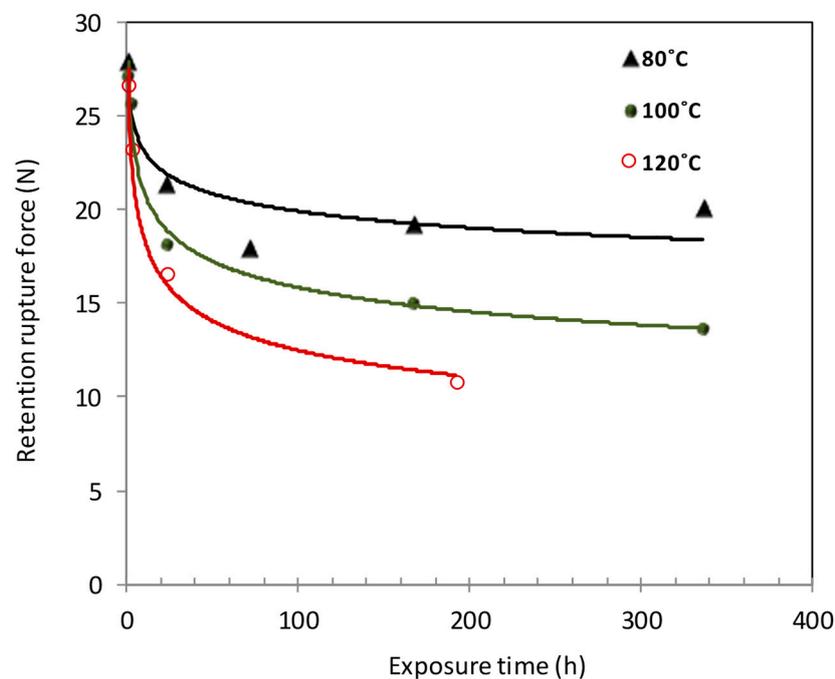
309
310   **Figure 6**   Variation of tensile force of BRC at different temperatures as a function of exposure time.
311
312   The definition of the end-used service lifetime of the material is still a subject in question in the
313   literature. However, the assumption proposed by Rachid *et al.*[67] in which the material is considered
314   run out when there is a reduction of about 50 % of tensile force seems to be acceptable. Here, were
315   calculated the service life time for each aging temperature, using an empirical regression proposed
316   method By El Aidani *et al.* [16, 67]. These lifetime values were exploited from Arrhenius curve, as
317   shown in Figure 7, by plotting the logarithm of the lifetimes as a function of the inverse of the exposed
318   temperatures. This Figure shows a good agreement with the *Arrhenius* model with high linear
319   correlation coefficient ($R^2 = 0.95$). This indicates that the effect of thermal treatment between 80 and
320   120 °C on tensile force of BRC can be satisfactorily described by the Arrhenius model, which can
321   therefore be used to predict the lifetime in this range of temperatures. The results of service life time
322   of BRC can be found in Figure 6. An activation energy value of 157 kJ.mol^{-1} was obtained from the

323 Arrhenius curve. That means, at 80 °C, the mechanical properties of BRC remains acceptable till 344
324 days while it drops to about 2 days at 120 °C.

325

Insert table:

Exposure temperature (°C)	Service lifetime (h)
80	8265.5
100	164.7
120	46.4

Plot equation: $y = 18.943x - 44.97$, $R^2 = 0.95$

326

327 **Figure 7**   Extrapolation of Arrhenius plot of BRC membrane based on tensile force. Insert:
328 Predicted values of service lifetime, calculated from Arrhenius plot based on tensile force at different
329 temperature.

4. Conclusions

331   The effect of temperature with and without MWFs on the evolution of mechanical and physico-
332 chemical descriptors as well as structure of BRC is investigated. The Mooney-Rivlin's theory is used
333 to determine the changes of physical and chemical bonds and the viscoelastic behavior of BRCs when
334 they are in contact with a MWFs at high temperature via the determination of the elastic constant C_1
335 and C_2 at different temperatures ranging from 80 °C to 120 °C. The results show that temperature and
336 MWFs lead to the decrease of elastic constant C_2, suggesting a decrease of the force of cohesion of
337 polymer network. When BRC membranes are in contact with MWFs at high temperature, the
338 irreversible behavior, related to intrinsic property of elastomers, is missing and significant changes
339 in mechanical properties of material are observed.

340   The temperature is found to be accelerated the degradation process and the loss of mechanical
341 properties of material was more pronounced at high temperature. The decrease of elasticity and
342 reduction of the glass transition temperature of BRC is also observed, implying that BRC is not
343 appropriated to use in oily working conditions, particularly in high temperature. In this case, gloves
344 making from BRC must be changed more frequently to ensure an adequate protection level against
345 mechanical and chemical risks. This work provides also useful information for rubber manufacturers
346 to better understand the physicochemical degradation phenomena of their products under oily
347 working conditions and thus improve the products quality.

348 **Author Contributions:** P.N.T has planned, supervised the works and written the manuscript. E.T has realized
349 the experiments and participated to explain results. T.A.N. participated to edit the manuscript.

Conflicts of Interest: The authors declare no conflict of interest.

5. References

1. Youssf, O., et al., *Cyclic Performance of Steel–Concrete–Steel Sandwich Beams with Rubcrete and LECA Concrete Core.* Journal of Composites Science, 2019. **3**(1): p. 5.

2. Youssf, O., et al., *Influence of Mixing Procedures, Rubber Treatment, and Fibre Additives on Rubcrete Performance.* Journal of Composites Science, 2019. **3**(2): p. 41.

3. Aguilar-Bolados, H., et al., *Removal of Surfactant from Nanocomposites Films Based on Thermally Reduced Graphene Oxide and Natural Rubber.* Journal of Composites Science, 2019. **3**(2): p. 31.

4. Nohilé, C., P.I. Dolez, and T. Vu-Khanh, *Mechanical and Chemical Effects of Solvent Swelling on Butyl Rubber.* 2010: p. 527-534.

5. Ebnesajjad, S., *8 - Characteristics of Adhesive Materials*, in *Handbook of Adhesives and Surface Preparation*, S. Ebnesajjad, Editor. 2011, William Andrew Publishing: Oxford. p. 137-183.

6. G. Pape, P., *15 - Adhesion Promoters*, in *Handbook of Adhesives and Surface Preparation*, S. Ebnesajjad, Editor. 2011, William Andrew Publishing: Oxford. p. 369-386.

7. Rabilloud, G., *12 - Adhesives for Electronics*, in *Handbook of Adhesives and Surface Preparation*, S. Ebnesajjad, Editor. 2011, William Andrew Publishing: Oxford. p. 259-299.

8. Rabilloud, G., *9 - Heat-Resistant Adhesives*, in *Handbook of Adhesives and Surface Preparation*, S. Ebnesajjad, Editor. 2011, William Andrew Publishing: Oxford. p. 185-220.

9. Fabris, H.J. and W.G. Knauss, *Synthetic Polymer Adhesives.* 1989: p. 131-177.

10. Haworth, J.P. and F.P. Baldwin, *Butyl Rubber Properties and Compounding.* Industrial & Engineering Chemistry, 1942. **34**(11): p. 1301-1308.

11. Ford, F.P. and A.M. Gessler, *Some Properties of Butyl Rubber-Carbon Black Systems.* Industrial & Engineering Chemistry, 1952. **44**(4): p. 819-824.

12. Yu, B.-C., et al., *A new approach for recycling waste rubber products in Li–S batteries.* Energy & Environmental Science, 2017. **10**(1): p. 86-90.

13. Xu, W. and S.S. Que Hee, *Permeation of a Metalworking Fluid Through a Latex Glove Under Field Use Conditions.* Bulletin of Environmental Contamination and Toxicology, 2009. **84**(1): p. 5.

14. Xu, W. and S.S. Que Hee, *Swelling of four glove materials challenged by six metalworking fluids.* Arch Environ Contam Toxicol, 2008. **54**(1): p. 1-8.

15. Nguyen-Tri, P., et al., *Swelling behavior of polymeric membranes to metalworking fluids.* Journal of Applied Polymer Science, 2018. **135**(3): p. 45717.

16. El Aidani, R., et al., *Photochemical aging of an e-PTFE/NOMEX® membrane used in firefighter protective clothing.* Polymer Degradation and Stability, 2013. **98**(7): p. 1300-1310.

17. Nguyen-Tri, P., et al., *Chemical ageingaging of a polyester nonwoven membrane used in aerosol and drainage filter.* Polymer Degradation and Stability, 2014. **101**: p. 71-80.

18. Nguyen, T.V., et al., *Accelerated degradation of water borne acrylic nanocomposites used in outdoor protective coatings.* Polymer Degradation and Stability, 2016. **128**: p. 65-76.

392   19.   Nguyen, T.P., *Nanoscale analysis of the photodegradation of Polyester fibers by AFM-IR* Journal of
393   Photochemistry and Photobiology A: Chemistry, 2018. **Accepted**.

394   20.   Nguyen, T.V., et al., *Stability of acrylic polyurethane coatings under accelerated aging tests and natural*
395   *outdoor exposure: The critical role of the used photo-stabilizers.* Progress in Organic Coatings, 2018. **124**: p.
396   137-146.

397   21.   Nguyen-Tri, P., et al., *Nanocomposite Coatings: Preparation, Characterization, Properties, and Applications.*
398   International Journal of Corrosion, 2018. **2018**: p. 1-19.

399   22.   Nguyen-Tri, P. and R.E. Prud'homme, *Nanoscale analysis of the photodegradation of polyester fibers by*
400   *AFM-IR.* Journal of Photochemistry and Photobiology A: Chemistry, 2019. **371**: p. 196-204.

401   23.   Nguyen-Tri, P., et al., *Recent progress in the preparation, properties and applications of superhydrophobic*
402   *nano-based coatings and surfaces: A review.* Progress in Organic Coatings, 2019. **132**: p. 235-256.

403   24.   Ouellet-Plamondon, P.N.T.S.R.C., *Nanomaterials-Based Coatings : Fundamentals and Applications.* Vol. 1.
404   2019: Elsevier. 474.

405   25.   Tri Phuong, N., V. Gilbert, and B. Chuong, *Preparation of Recycled Polypropylene/ Organophilic Modified*
406   *Layered Silicates Nanocomposites Part I: The Recycling Process of Polypropylene and the Mechanical*
407   *Properties of Recycled Polypropylene/Organoclay Nanocomposites.* Journal of Reinforced Plastics and
408   Composites, 2008. **27**(18): p. 1983-2000.

409   26.   Nguyen Tri, P. and V. Gilbert, *Non-isothermal Crystallization Kinetics of Short Bamboo Fiber-reinforced*
410   *Recycled Polypropylene Composites.* Journal of Reinforced Plastics and Composites, 2010. **29**(17): p. 2576-
411   2591.

412   27.   Nguyen Tri, P., C. Sollogoub, and A. Guinault, *Relationship between fiber chemical treatment and*
413   *properties of recycled pp/bamboo fiber composites.* Journal of Reinforced Plastics and Composites, 2010.
414   **29**(21): p. 3244-3256.

415   28.   Boukehili, H. and P. Nguyen-Tri, *Helium gas barrier and water absorption behavior of bamboo fiber*
416   *reinforced recycled polypropylene.* Journal of Reinforced Plastics and Composites, 2012. **31**(23): p. 1638-
417   1651.

418   29.   Nguyen Tri, P., A. Guinault, and C. Sollogoub, *Élaboration et propriétés des composites polypropylène*
419   *recyclé/fibres de bambou.* Matériaux & Techniques, 2012. **100**(5): p. 413-423.

420   30.   Triki, E., et al., *Investigation of tearing mechanisms of woven textile.* Polymer Composites, 2012. **33**(9): p.
421   1578-1585.

422   31.   Triki, E., et al., *Mechanics and mechanisms of tear resistance of woven fabrics.* Theoretical and Applied
423   Fracture Mechanics, 2012. **61**: p. 33-39.

424   32.   Tri, P.N., et al., *Crystallization behavior of poly(lactide)/poly(β-hydroxybutyrate)/talc composites.* Journal of
425   Applied Polymer Science, 2013. **129**(6): p. 3355-3365.

426   33.   Triki, E., et al., *Combined puncture/cutting of elastomer membranes by pointed blades: Characterization of*
427   *mechanisms.* Journal of Applied Polymer Science, 2015. **132**(26): p. n/a-n/a.

428   34.   Azizi, S., et al., *Electrical and thermal phenomena in low-density polyethylene/carbon black composites near*
429   *the percolation threshold.* Journal of Applied Polymer Science, 2018: p. 47043.

430   35.   Azizi, S., et al., *Electrical and thermal conductivity of ethylene vinyl acetate composite with graphene and*
431   *carbon black filler.* Polymer Testing, 2018. **72**: p. 24-31.

432   36.   Nguyen Tri, P. and R.E. Prud'homme, *Crystallization and Segregation Behavior at the Submicrometer Scale*
433   *of PCL/PEG Blends.* Macromolecules, 2018. **51**(18): p. 7266-7273.

434   37.   Satyabrata, M.T., Anh Nguyen; Phuong, Nguyen-Tri;, *Noble Metal-Metal Oxide Hybrid Nanoparticles.*
435   Vol. 1. 2018: Elsevier.

436   38.   Duc Chinh, V., et al., *Synthesis of Gold Nanoparticles Decorated with Multiwalled Carbon Nanotubes (Au-*
437   *MWCNTs) via Cysteaminium Chloride Functionalization.* Scientific Reports, 2019. **9**(1): p. 5667.

438   39.   Nguyen Tri, P., et al., *Antibacterial Behavior of Hybrid Nanoparticles.* 2019: p. 141-155.

439   40.   Nguyen Tri, P., et al., *Methods for Synthesis of Hybrid Nanoparticles.* 2019: p. 51-63.

440   41.   Nguyen-Tri, P., V. Nguyen, and T. Nguyen, *Biological Activity and Nanostructuration of Fe3O4-Ag/High*
441   *Density Polyethylene Nanocomposites.* Journal of Composites Science, 2019. **3**(2): p. 34.

442   42.   Ben Hassine, M., et al., *Time to failure prediction in rubber components subjected to thermal ageing: A*
443   *combined approach based upon the intrinsic defect concept and the fracture mechanics.* Mechanics of
444   Materials, 2014. **79**: p. 15-24.

445   43.   Syed, I.H., et al., *Nonlinearity in the Mechanical Response of Rubber as Investigated by High-Frequency*
446   *DMA.* Polymers (Basel), 2019. **11**(4).

447   44.   Xiang, K., et al., *Investigation on the thermal oxidative aging mechanism and lifetime prediction of butyl*
448   *rubber.* Macromolecular Research, 2013. **21**(1): p. 10-16.

449   45.   Haghtalab, A. and S. Rahimi, *Study of viscoelastic properties of nanocomposites of SiO2-acrylonitrile-*
450   *butadiene-styrene.* Journal of Applied Polymer Science, 2013. **127**(6): p. 4318-4327.

451   46.   Lewicki, J.P., et al., *Degradative Thermal Analysis and Dielectric Spectroscopy Studies of Aging in*
452   *Polysiloxane Nanocomposites.* 2009. **1004**: p. 239-254.

453   47.   Rivlin, R.S., *Large Elastic Deformations of Isotropic Materials. IV. Further Developments of the General*
454   *Theory.* Philosophical Transactions of the Royal Society A: Mathematical, Physical and Engineering
455   Sciences, 1948. **241**(835): p. 379-397.

456   48.   Rivlin, R.S., *Large Elastic Deformations of Isotropic Materials. I. Fundamental Concepts.* Philosophical
457   Transactions of the Royal Society A: Mathematical, Physical and Engineering Sciences, 1948. **240**(822):
458   p. 459-490.

459   49.   Arimoto, H., *α–γ Transition of nylon 6.* Journal of Polymer Science Part A: General Papers, 1964. **2**(5): p.
460   2283-2295.

461   50.   Slichter, W.P., *Molecular motion in polyamides.* Journal of Polymer Science, 1959. **35**(128): p. 77-92.

462   51.   Hagen, R., L. Salmén, and B. Stenberg, *Effects of the type of crosslink on viscoelastic properties of natural*
463   *rubber.* Journal of Polymer Science Part B: Polymer Physics, 1996. **34**(12): p. 1997-2006.

464   52.   Gordon, M., *The Physics of Rubber Elasticity (Third Edition). L. R. G. Treloar, Clarendon Press, Oxford. 1975*
465   *pp. xii + 370. Price: £14.00.* British Polymer Journal, 1976. **8**(1): p. 39-39.

466   53.   Sombatsompop, N., *Investigation of Swelling Behavior of NR Vulcanisates.* Polymer-Plastics Technology
467   and Engineering, 1998. **37**(1): p. 19-39.

468   54.   Mark, J.E., *Experimental Determinations of Crosslink Densities.* Rubber Chemistry and Technology, 1982.
469   **55**(3): p. 762-768.

470   55.   Priss, L.S., *Molecular origin of constants in the theory of rubber-like elasticity considering network chains*
471   *steric interaction.* Pure and Applied Chemistry, 1981. **53**(8): p. 1581-1596.

472   56.   Mark, J.E., *The Constants 2C1and 2C2in Phenomeno-Logical Elasticity Theory and Their Dependence on*
473   *Experimental Variables.* Rubber Chemistry and Technology, 1975. **48**(3): p. 495-512.

474   57.   Ha-Anh, T. and T. Vu-Khanh, *Prediction of mechanical properties of polychloroprene during thermo-*
475   *oxidative aging.* Polymer Testing, 2005. **24**(6): p. 775-780.

476   58.   Gumbrell, S.M., L. Mullins, and R.S. Rivlin, *Departures of the elastic behaviour of rubbers in simple*

477   *extension from the kinetic theory.* Transactions of the Faraday Society, 1953. **49**(0): p. 1495-1505.

478   59.   Allen, G., et al., *Thermodynamics of rubber elasticity at constant volume.* Transactions of the Faraday

479   Society, 1971. **67**(0): p. 1278-1292.

480   60.   Dutta, N.K., D. Khastgir, and D.K. Tripathy, *The effect of carbon black concentration on the dynamic*

481   *mechanical properties of bromobutyl rubber.* Journal of Materials Science, 1991. **26**(1): p. 177-188.

482   61.   García, M., I. Garmendia, and J. García, *Influence of natural fiber type in eco-composites.* Journal of

483   Applied Polymer Science, 2008. **107**(5): p. 2994-3004.

484   62.   Ali, S., et al., *Thermal and Thermo-Mechanical Behavior of Butyl based Rubber Exposed to Silicon Oil at*

485   *Elevated Temperature.* Journal of the Chemical Society of Pakistan, 2013. **35**(6): p. 1437-1444.

486   63.   Barrere, C. and F. Dal Maso, *Résines époxy réticulées par des polyamines : structure et propriétés.* Revue de

487   l'Institut Français du Pétrole, 2006. **52**(3): p. 317-335.

488   64.   Fox, T.G. and P.J. Flory, *Second-Order Transition Temperatures and Related Properties of Polystyrene. I.*

489   *Influence of Molecular Weight.* Journal of Applied Physics, 1950. **21**(6): p. 581-591.

490   65.   G K Kannan, L.V.G., L Nirmala and N S Kumar, *Thermal ageing studies of bromo-butyl rubber used in*

491   *NBCpersonal protective equipment.* Journal of Scientific & Industrial Research, 2010. **69**: p. 841-849.

492   66.   Grandcoin, J., A. Boukamel, and S. Lejeunes, *A micro-mechanically based continuum damage model for*

493   *fatigue life prediction of filled rubbers.* International Journal of Solids and Structures, 2014. **51**(6): p. 1274-

494   1286.

495   67.   El Aidani, R., P.I. Dolez, and T. Vu-Khanh, *Effect of thermal aging on the mechanical and barrier properties*

496   *of an e-PTFE/Nomex® moisture membrane used in firefighters' protective suits.* Journal of Applied Polymer

497   Science, 2011. **121**(5): p. 3101-3110.